



Magnetism and ferromagnetic loss in Ni–W textured substrates for coated conductors

A.O. Ijaduola^a, J.R. Thompson^{a,b,*}, A. Goyal^b, C.L.H. Thieme^c, K. Marken^d

^a Department of Physics, University of Tennessee, Knoxville, TN 37996-1200, USA

^b Oak Ridge National Laboratory, Bldg. 3115, P.O. Box 2008, Oak Ridge, TN 37831-6061, USA

^c American Superconductor Corp., Westborough, MA 01581, USA

^d Oxford Instruments Superconducting Technology, Carteret, NJ 07008, USA

Received 16 October 2003; received in revised form 4 December 2003; accepted 9 December 2003

Abstract

A study has been conducted on the magnetic properties of a series of biaxially textured $\text{Ni}_{1-x}\text{W}_x$ materials with compositions $x = 0, 3, 5, 6,$ and 9 at.% W. These materials are important as substrates for “RABiTS”-type coated conductors that incorporate high temperature superconductors for current transport. The quasi-static dc and ac hysteretic loss W was determined to support estimates of the ferromagnetic contribution to the overall ac loss in potential ac applications. The alloys were prepared by either vacuum casting or powder metallurgy methods, and the hysteretic loss tended to be lower in materials that were recrystallized at higher temperatures. Some samples were progressively deformed (0.4% bending strain) to simulate winding operations; this increased the hysteretic loss, as did sample cutting operations that create localized damage. In ac magnetization measurements, the effects of ac frequency and dc bias field on the ferromagnetic loss were determined.

© 2003 Elsevier B.V. All rights reserved.

PACS: 85.25.Am; 84.71.Mn; 75.50.Cc

Keywords: Ni–W alloys; Magnetization; Hysteretic loss; Coated conductor applications

1. Introduction

High temperature superconductors (HTS) are fascinating materials with great fundamental interest and significant technological potential, one of which is the development of tapes and cables for low

loss conduction of high density electric currents. Issues arising from the “weak-link” intergrain current transport have led to the development of different methods for their fabrication. The rolling assisted biaxially textured substrates (RABiTS) [1–4], IBAD [5–8] and the ISD [9,10] methods are the most recent methods being used to create a substrate on which highly textured HTS with low angle grain boundaries can conduct large intergrain currents. The Ni–W alloys studied in this work are well suited as the base material for RABiTS applications.

* Corresponding author. Address: Oak Ridge National Laboratory, Bldg. 3115, P.O. Box 2008, Oak Ridge, TN 37831-6061, USA. Tel.: +1-865-574-0412; fax: +1-865-574-6263.

E-mail address: jrt@utk.edu (J.R. Thompson).

Nickel, which is more amenable to the thermo-mechanical processing that produces biaxial texturing, was initially used for RABiTS conductors. However, its ferromagnetism (FM), with a Curie temperature of 627 K and a saturation magnetization of 57.5 emu/g at $T = 0$ K, is considered undesirable. Moreover, its usage in alternating current (ac) applications can lead to significant hysteretic losses that add to the usual ac losses in the superconductor. Consequently, suitable alloys with reduced FM need to be developed. Moreover, substrates which are significantly stronger than nickel are required for practical applications. In earlier work, we investigated certain magnetic properties of a series of Ni–Cr materials that were biaxially textured [11]. This present work deals more extensively with the alloy series Ni–W, highlighting their magnetic properties. The addition of W to Ni significantly increases the yield strength of the substrate as well as reduces the magnetism [12]. Moreover, deposition of high quality, epitaxial oxide buffer layers directly on NiW substrates is possible [12]. These advantages have led at least two commercial manufacturers to adopt Ni–W materials for use in production of prototype coated conductors.

2. Experimental

$\text{Ni}_{1-x}\text{W}_x$ materials with nominal compositions $x = 0, 3, 5, 6,$ and 9 at.% W were used. The alloys were formed by either vacuum melting or by powder metallurgy methods. The starting alloys were then subjected to thermo-mechanical processing (a series of rolling deformations and heat treatment) to produce the desired (100) [100] cube texture, i.e., with one crystallographic {100} axis oriented perpendicular to the plane of the tape and with another directed along the tape axis. In the final step, the alloys were recrystallized by annealing at temperatures in the range $T_{\text{ann}} = 950\text{--}1150$ °C for the vacuum cast materials and 1300 °C for the powder metallurgy alloys; the maximum temperature is limited by the need to avoid secondary recrystallization, which destroys the desired biaxial texturing.

For the magnetic studies, a sample of tape, with typical dimensions of $3\text{--}4$ mm \times $3.5\text{--}4$ mm and

thickness of $50\text{--}75$ μm , was mounted in a SQUID-based magnetometer, either a Quantum Design model MPMS-7 or a model XL with ac capabilities. The tape was vertical with the magnetic field H applied parallel to the sample's surface, in order to minimize demagnetizing effects. Temperatures ranged from 5 to 375 K in fields up to 15 kOe. We measured both the isothermal mass magnetization $M(H)$ at different fixed temperatures and $M(T)$ in fixed field. For the FM loss studies, we measured one complete loop of the quasi-static dc magnetization $M(H)$, starting from field $+H_{\text{max}}$ and sweeping to field $-H_{\text{max}}$, then back to field $+H_{\text{max}}$. This process was repeated at progressively higher field amplitudes H_{max} in the range $5\text{--}400$ Oe. For example, in a 100 Oe cycle, ($H_{\text{max}} = 100$ Oe) the sample was first "exercised" by applying a magnetic field $H = +100, -100, +100$ and -100 Oe, to simulate several cycles of ac field in an application and to establish the steady state ferromagnetic response. Then the loop $M(H)$ (in units of $\text{G cm}^3/\text{g}$) was measured, sweeping the field in small increments from $+100$ to -100 Oe and back to $+100$ Oe. In any conductor configuration, the field excursion H_{max} will increase with the amplitude of the ac current, with a geometry-dependent proportionality [13]. Measurements of FM loss were done at $T = 50$ and 77 K.

In some cases, the ac magnetization was measured, in order to see if the FM loss/cycle depended on frequency. Frequencies ranged from 2.5 to 600 Hz, with ac field amplitudes h_{ac} up to 6.8 Oe peak. In one case, a bias dc field was applied parallel to the ac field to assess its influence. For the deformation studies, we used a common bending strain of 0.4% for all the samples deformed. Using the formula

$$\text{bending strain} = \frac{\text{thickness of sample}}{\text{diameter of mandrel}},$$

an appropriate mandrel was used to deform each of the samples. A sample was wrapped around the mandrel and then flattened to complete a half-cycle of deformation; when reverse wrapped and again flattened, the tape completed one complete deformation cycle. The objective of this bending study was to simulate the work hardening that might be encountered during handling or fabrica-

tion of electrical equipment, e.g., during winding operations. In addition, we determined the increase in loss associated with cutting the Ni–W alloy substrate, as might be encountered in slitting operations following final fabrication of a coated conductor. Finally, the effect of temperature cycling was investigated for one sample, by dipping it in liquid nitrogen, warming it to room temperature, and then immersing it again. This thermal cycle was repeated eight times, after which the FM loss was remeasured in a 400 Oe cycle at 77 K.

3. Results and discussion

For an overall perspective, Fig. 1 shows the mass magnetization M plotted versus applied field H for all compositions studied. The measurements were done at $T = 5$ K in fields H up to 10 kOe, in order to obtain the saturation magnetization M_{sat} . The values of M_{sat} steadily decrease with the addition of tungsten. This is clearly seen in Fig. 2, a plot of M_{sat} versus W-content x . The figure reveals a variation with x that is very nearly linear, similar to that observed in Ni–Cr alloys [14,11]. A linear extrapolation to $M_{\text{sat}} = 0$ intersects at a critical W-concentration $x_c = 9.55 \pm 0.40$ at.%. Long ago, this alloy system was studied by Marian [15] and subsequently reported in Bozorth's book

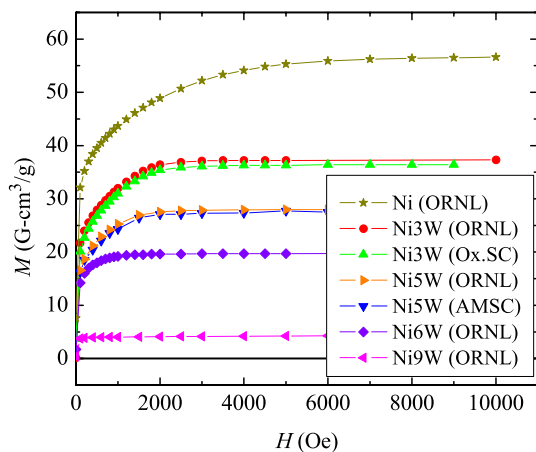


Fig. 1. The magnetization M of $\text{Ni}_{1-x}\text{W}_x$ alloys versus applied magnetic field H , for each composition studied; annotations in figure show W-content x in atomic percent, e.g., Ni3W = 3 at.%. Measurements were done at $T = 5$ K.

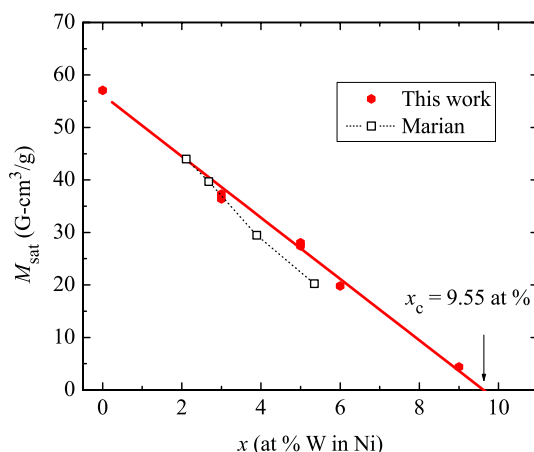


Fig. 2. Variation of saturation magnetization of $\text{Ni}_{1-x}\text{W}_x$ alloys with W-content x , including values obtained here and those reported by Marian [15]. The line is a linear dependence fitted to the present data and extrapolated to the critical concentration x_c .

[16] and still later in a data compilation [17]. The data of Marian are included in Fig. 2.

We determined the Curie temperature T_c for several alloys from temperature-dependent measurements of $M(T)$. The analysis was based on the relation that the spontaneous magnetization varies with temperature as $M \propto (T_c - T)^\beta$ with $\beta \approx 1/3$ for a 3D Heisenberg magnet [18]. In approximating the spontaneous magnetization by the bulk signal, we ignore all data very close to T_c due to the influence of the applied field. The process is illustrated in Fig. 3, which shows M^3 plotted against T for two alloys, Ni–5at.%W and Ni–6at.%W. The substantial region of linearity shows that the “critical point” relation given above describes the system rather well. The Curie temperature was obtained by a linear extrapolation to $M^3 = 0$. The resulting values of T_c are presented in Fig. 4 as a function of W-concentration x . Again, the values of Marian [15] are included for comparison. As with the saturation magnetization M_{sat} , we observe a nearly linear decrease with x ; a linear extrapolation to $T_c = 0$ gives a value for the critical concentration $x_c = 9.75 \pm 0.40$ at.%, which is consistent within experimental error with the result from M_{sat} . This implies, perhaps more fundamentally, that M_{sat} and T_c are proportional in these

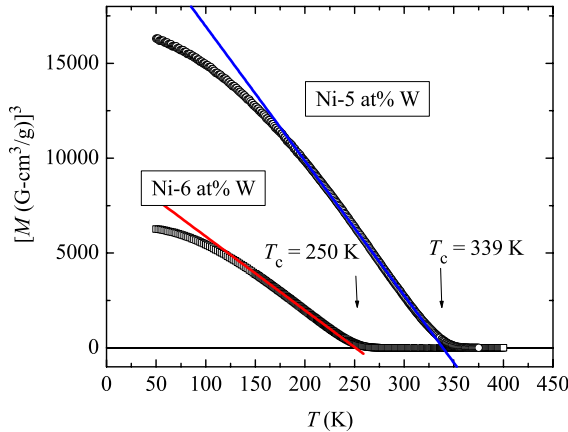


Fig. 3. A plot of M^3 versus temperature T for Ni-5at.%W and Ni-6at.%W. Straight lines show the extrapolation to $M = 0$ used to define Curie temperature.

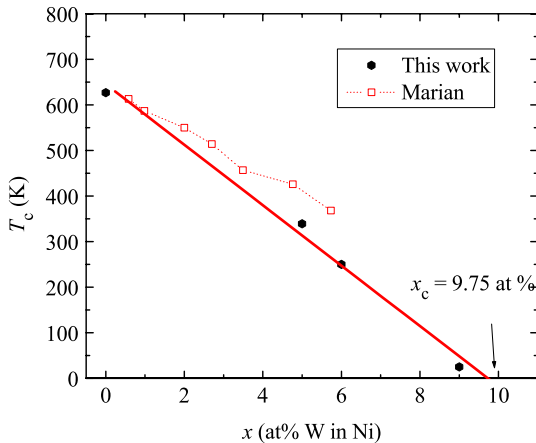


Fig. 4. Dependence of Curie temperature of $\text{Ni}_{1-x}\text{W}_x$ alloys on W-content x , with present results and those of Marian [15]. The straight line extrapolates to the critical concentration x_c .

Ni–W (and Ni–Cr) alloys. Table 1 lists these two parameters for the present samples.

Next, we consider the hysteretic energy loss in these ferromagnetic Ni materials. To illustrate some essential features, we show in Fig. 5 several plots of magnetization M versus H for a rather lossy sample of electroplated Ni, at $T = 120$ K. Included are curves for cycles with $H_{\max} = 100, 200, 400$ and 800 Oe. Qualitatively, it is clear that the area inside the loop increases as the field excursion increases, and then saturates when the material becomes reversible in sufficiently large

Table 1
Magnetic properties of Ni–W alloys

Material	M_{sat} (G cm ³ /g)	T_c (K)
Nickel	57.06	627
Ni-3at.%W	36.4–37.3	>420
Ni-5at.%W	27.4–28.0	339
Ni-6at.%W	19.8	250
Ni-9at.%W	4.36	25

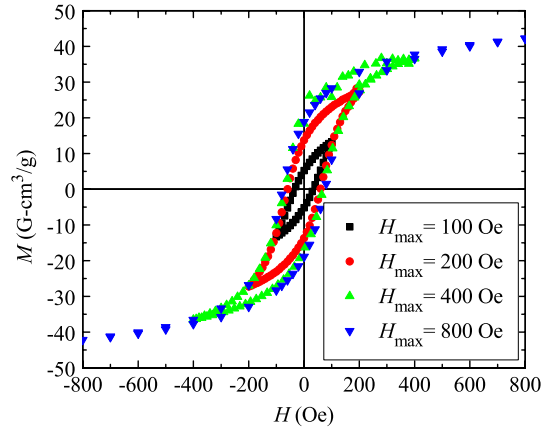


Fig. 5. The magnetization M versus H for lossy, electroplated Ni at a temperature of 120 K. The plot illustrates that the FM loss, $W = \int M dH = \text{loop area}$, increases with H_{\max} .

fields. This is the general behavior for the biaxially textured substrate materials also, but their loops are much more narrow and the changing area is less visible. To obtain the hysteretic energy loss/cycle W , we numerically integrate each $M(H)$ loop to obtain its area (in units of erg/g cycle). Many of these results are collected in Fig. 6, a plot of loss W versus field excursion H_{\max} . The general response of these soft ferromagnetic materials (coercive fields of a few Oe) is similar, with a *roughly* linear variation at low field amplitudes H_{\max} , followed by saturation at higher field amplitudes. As the temperature decreases, the loss W increases as might be expected, but only slightly between 77 and 50 K.

To better visualize some trends, we show in Fig. 7 the maximum FM energy loss/cycle W for each alloy as biaxially textured (no bending deformation), at $T = 77$ K. In particular, the histogram contains values of loss measured in 400 Oe cycles, with the materials listed in order of increasing W-content. Two qualitative trends can be discerned.

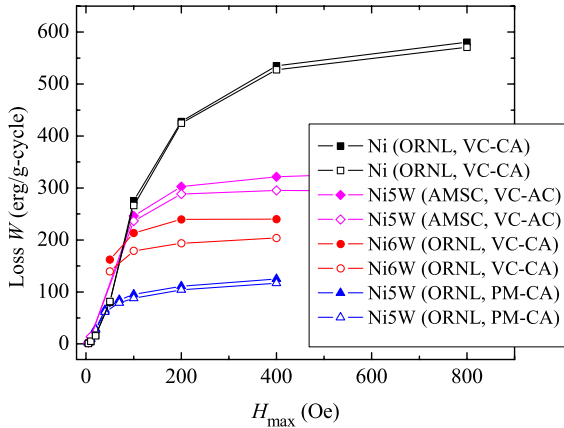


Fig. 6. Hysteric loss per cycle W as a function of field excursion H_{max} , for undeformed Ni, Ni-6at.%W and Ni-5at.%W materials at $T = 50$ K (filled symbols) or 77 K (open symbols). Loss increases roughly linearly with H_{max} , then saturates. Also, loss increases somewhat as T decreases. Samples were prepared by vacuum casting (VC) or powder metallurgy (PM); then recrystallized by annealing and cut-to-size (AC) or cut-to-size and then annealed (CA); annotations in figure show W-content x in atomic percent, e.g., Ni5W = 5 at.% W.

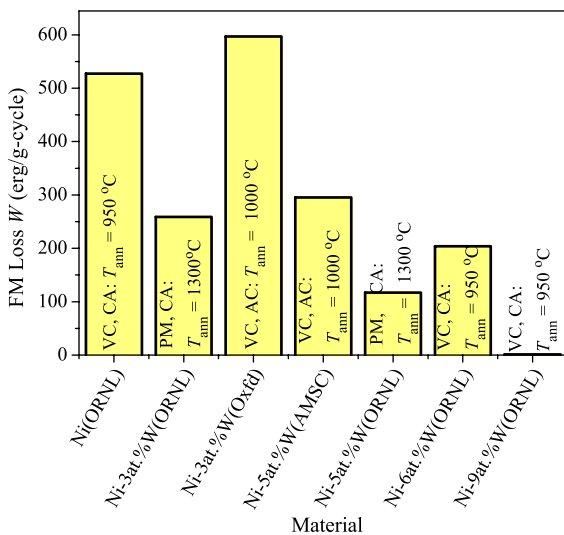


Fig. 7. Histogram showing maximum hysteric loss W of several samples. Alloys with same atomic composition have different values of FM losses due to different methods of preparation: alloys annealed at higher temperatures T_{ann} after cutting operations (CA) have lower FM losses; PM = powder metallurgy; VC = vacuum cast. Ni-9at.%W has an almost negligible loss.

First, the loss W generally decreases when tungsten is added. This is hardly surprising, for Ni-W at these compositions forms a solid solution (no precipitates or inclusions that could pin domain walls) and, as shown in Fig. 2, the saturation magnetization M_{sat} decreases approximately linearly with W-content. The Ni-9at.%W has negligible loss, as expected from the critical concentration of W in Ni. Let us recall, however, the loss depends not only on intrinsic material properties like M_{sat} , but also on extrinsic features like the density of defects that pin domain walls. Second, then, we observe that the FM loss for materials with similar compositions tends to be lower for those annealed (recrystallized) at higher temperatures. For example, the Ni-5at.%W powder metallurgy material has lower loss than the vacuum cast 6 at.%W alloy, where each was annealed—given its final heat treatment—after cutting to size (noted as “CA”). This second observation most likely originates from the higher annealing temperatures (~ 1300 °C) that could be used with the PM-based alloys (without inducing unwanted secondary recrystallization), compared with vacuum cast materials recrystallized near ~ 1000 °C. Qualitatively, annealing at higher temperatures should lead to a lower density of dislocations and related structural defects. Indeed, dislocations are reported to be a primary source of pinning that impedes domain wall motion in Ni [19] and one may expect similar effects in these dilute Ni-W alloys. Grain boundaries also act as pin domain walls, but the present materials are all strongly textured with small angle grain boundaries that constitute a “wall” of dislocation cores. With similar mean grain sizes, this implies that the differences between materials arise mostly from other features.

In practice, another source of defects in the materials is cutting, which creates localized damage near the severed edge. To assess this effect, we investigated the loss in Ni-5at.%W samples that were either cut-to-size (4 mm \times 4 mm) first and then annealed (“CA”) or annealed for recrystallization and then cut-to-size (“AC”). The results are shown in Fig. 8 as a plot of loss W versus H_{max} all at $T = 77$ K. Clearly, work-hardened edges induced by sample cutting significantly increased

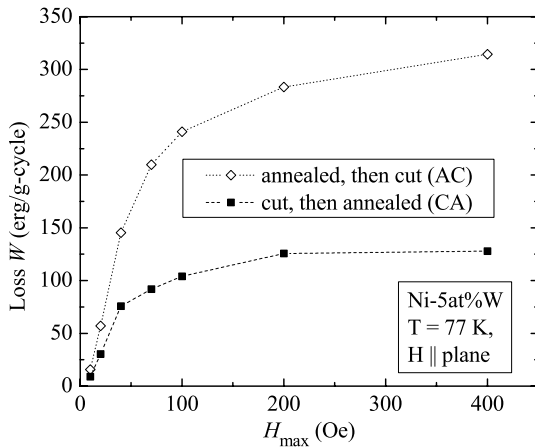


Fig. 8. Effect of cutting on the ferromagnetic loss per cycle W , shown as a function of field excursion H_{\max} . The samples of undeformed Ni-5at.%W materials (prepared by vacuum casting, AMSC) were cut and then annealed (CA) or first recrystallized and then cut (AC).

the ferromagnetic loss from its low initial level, e.g., increasing the coercive field H_c from 1 to 3 Oe. Losses in the vacuum-cast CA alloy are nearly identical to those measured in CA powder metallurgy alloys, all containing 5 at.% W. In a separate experiment, we cut a 4×4 mm CA sample into three pieces, severing it with a razor blade on a hard tungsten plate. This operation added 16 mm of freshly cut edges and added to the maximal loss at a rate of 1.2 erg/cycle per cm of cut edge (for this Ni-5at.%W material with 75 μm thickness). These combined results show that preparation and handling of the Ni-W alloy substrates play a prominent role in determining their hysteretic losses, as should be expected for this extrinsic property.

Next we consider the impact of bending deformation on the ferromagnetic loss/cycle. For this study, we used pure Ni, Ni-3at.%W and Ni-5at.%W materials. Each of these samples was deformed controllably by applying 0.4% bending strain, as described earlier. Fig. 9 shows how the loss W increases with the number of half-cycles of bend, for Ni-3at.%W and Ni-5at.%W materials. This figure shows the maximal FM loss/cycle, as observed in field cycles with $H_{\max} = 400$ Oe. For all alloys, the hysteretic loss increased with number of cycles of deformation, with the biggest jump in loss coming from the first half-step of deforma-

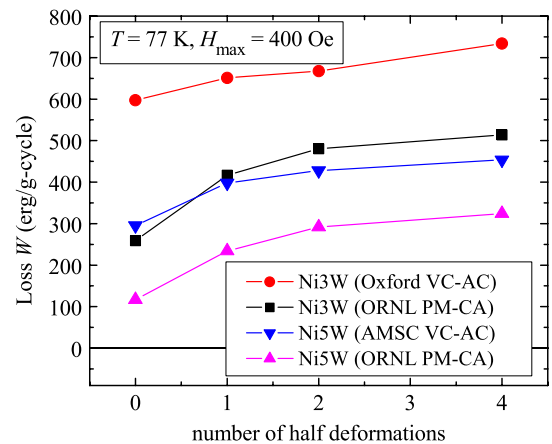


Fig. 9. Hysteretic loss per cycle for Ni-3at.%W and Ni-5at.%W as a function of number of half-cycles of deformation. Loss increases with number of cycles of deformation (0.4% bending strain). VC = vacuum cast; PM = powder metallurgy; AC = recrystallized and cut-to-size; CA = cut-to-size and then annealed.

tion. A bending strain of 0.4% lies near the limit tolerated by the superconductive coating in fully fabricated materials [20,21].

A check was made for adverse effects of temperature cycling, using a free-standing vacuum cast Ni-5at.%W sample as biaxially textured. Eight thermal cycles of $T = 300\text{--}77\text{--}300$ K changed the FM loss only slightly, from $W = 295$ to 302 erg/g cycle. From this, we can say that FM loss is essentially unaffected by temperature cycling.

In ac magnetic measurements, a small oscillatory magnetic field is applied and the induced sample moment is time-dependent, unlike the dc measurements where the sample moment is constant during the measurement time. Such measurements can be very sensitive to small changes in $M(H)$. The ac susceptibility, $\chi = dM/dH$ is the (local) slope of the $M(H)$ curve and it is frequently the quantity of interest in ac magnetometry. More generally, however, a measurement of an ac magnetic moment yields two quantities: the magnitude of the moment $|m|$ and its phase shift ϕ , relative to the drive signal. Alternatively, one can consider the in-phase or real component m' and an out-of-phase, or imaginary, component m'' . For ferromagnets, an irreversible domain wall movement appears as a finite dissipative component m'' . Values for the FM loss were obtained from the expression

$$W = \pi \times h_{ac} \times M'' ,$$

where M'' is the out-of-phase mass magnetization and h_{ac} is the amplitude of the applied ac field [22]. The SQUID magnetometer provides an ac field up to 6.8 Oe and its frequency range is from 0.001 to 1000 Hz. Comparing experimental values for loss W from ac and dc measurements gave good agreement between the two methods, although this could only be done for small fields, up to 6.8 Oe.

We used this ac capability to investigate the relationship between the FM loss/cycle and the frequency of the applied field. This is important because some potential applications for coated conductors in specialized electrical equipment, e.g., airborne generators and devices, have operating frequencies well above the usual 50–60 Hz of the power grid. As seen in Fig. 10, the loss/cycle W was found to be independent of the ac field frequency, at least for the small fields that were used. The figure shows results for vacuum cast Ni–5at.%W at 77 K subjected to field amplitudes $h_{ac} = 4$ and 6.8 Oe, for frequencies f up to 600 Hz. Here, there was no DC bias field and the sample had no bending deformation. The significant increase in loss with $h_{ac} = 6.8$ Oe compared with that at $h_{ac} = 4$ Oe occurs when the field amplitude h_{ac} or H_{max} is comparable with the coercive field H_c . Another potential loss mechanism is from eddy currents,

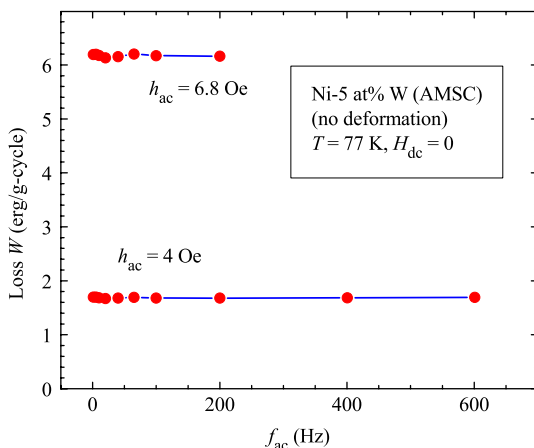


Fig. 10. FM loss as a function of applied ac frequency for two different fixed values of ac field. Loss per cycle is independent of frequency in the range shown.

which gives a nominally frequency-dependent but amplitude-independent loss. However, we estimate from the electrical resistivity and the magnetic permeability that the skin depth of this alloy is several millimeters, much larger than the sample thickness, meaning that eddy losses should be small relative to the FM loss, as observed.

Finally, we investigated the effect of a dc bias field, H_{dc} on the FM loss W for a fixed ac field amplitude and frequency. Similar superpositioning of ac and dc magnetic fields may arise in applications, e.g., in the stator of a motor. Fig. 11 shows the result obtained for an undeformed Ni–5at.%W at h_{ac} of 5 Oe and temperature of 77 K. The loss decreased rapidly as the bias field H_{dc} increased and reduced W to nearly zero for a dc field of ~ 50 Oe. This is readily understood as a consequence of the fact that a dc field can magnetize the sample into its region of magnetic reversibility (and eventually saturation). For the lossy electroplated Ni in Fig. 5, this region corresponds to dc fields $>\sim 400$ Oe; it occurs at lower fields for the more reversible biaxially textured and annealed Ni–W alloys, as can be seen in the inset to Fig. 11, where the material becomes reversible for fields exceeding ~ 70 –100 Oe.

Before closing, it is useful to provide some context for the FM properties of the substrate

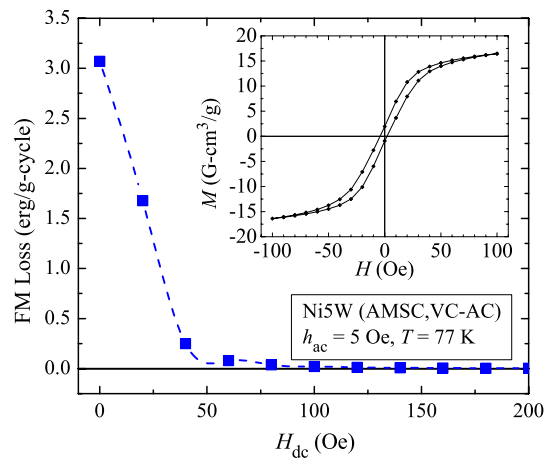


Fig. 11. Hysteretic loss for undeformed Ni–5at.%W versus dc bias field at temperature of 77 K and a fixed ac field of 5 Oe. Loss decrease drastically when alloy is magnetized into reversibility by dc bias field. Inset: magnetization of similarly annealed-and-cut (AC) Ni5W alloy.

materials, by comparing their FM loss with the hysteretic loss expected from the superconductor itself. As an example, let us consider a RABiTS tape that is 4 mm wide with a 75 μm thick metal substrate, which has a YBCO coating on one side giving a critical current $I_c = 100$ A. To estimate the superconductive energy loss, we use the theory of Norris [23], which applies to a long isolated conductor with an I_c that is independent of field. The theory (for elliptic geometry) provides a reasonably good description of the ac loss in YBCO coated conductors on Ni [24], on Hastelloy [25], and on some NiW-based architectures [13]. For a peak ac current $I_0 = I_c$ the Norris expression gives a loss per cycle per meter (SI units) of $L_c = (1/2\pi)\mu_0 I_0^2 = 2$ mJ/m cycle. For lower currents, Table 3 of Norris [23] shows that the losses are smaller by a factor of 3.2 at $I_0/I_c = 0.8$ and a factor of 9.4 at $I_0/I_c = 0.6$; the corresponding superconductive losses are $L_c = 0.63$ and 0.21 mJ/m cycle, respectively.

In this example, each meter of tape contains $0.3 \text{ cm}^3 = 2.7$ g of alloy substrate. For illustration, we use data for the Ni–5at.%W alloy (CA) in Fig. 6. To obtain the approximate field amplitude H_{max} , we approximate the tape by a thin strip with a uniformly distributed current, which (away from the edges) creates a field $B = \mu_0 I_0 / 2w$ (SI units), where “ w ” is the tape width. This field is in the plane of the tape, i.e., it has the same orientation as the field used for the quasi-static magnetic measurements.¹ The resulting fields ($H_{\text{max}} = 126$

and 94 Oe) produce similar FM hysteretic losses (92 and 86 erg/g cycle) of 0.025 and 0.023 mJ/m cycle at $I_0/I_c = 0.8$ and 0.6, respectively.

These FM losses constitute 4% and 10% of the total (superconductive plus ferromagnetic) loss at the respective current levels. The corresponding total dissipated power at 60 Hz is 122 mW/m at $I_0/I_c = 1$; 39 mW/m at the 0.8 level; and 14 mW/m at $I_0/I_c = 0.6$. For still lower current levels, the total power continues to decrease, while the FM loss becomes a progressively larger fraction of it. This example illustrates the magnitude of losses that might be encountered in power line applications. Clearly the dissipated power will be proportionately larger with higher operating frequencies and also with substrate materials that are deformed, cut, or otherwise damaged; on the other hand, both superconductive and FM losses could be reduced in conductor configurations with lower effective ac field amplitudes, e.g. possibly by grooving the conductor or coating both sides of the tape. Ultimately, the total loss will depend not only on the choice of substrate materials and operating conditions I_0/I_c , but also on the conductor and equipment layout that affects the ac field experienced by the conductor.

4. Conclusions

In summary, both the saturation magnetization M_{sat} and Curie temperature T_c decrease linearly with W-content x in $\text{Ni}_{1-x}\text{W}_x$ alloys (with $x = 0, 3, 5, 6,$ and 9 at.% W), with a critical concentration $x_c \approx 9.6$ at.% W. Generally, the FM hysteretic loss decreases as the concentration of W rises. The loss increases with magnetic field excursion H_{max} , at first almost linearly and then saturating at larger H_{max} . The loss is stable with temperature cycling. When subjected to shearing or bending deformation, (0.4% bending strain), the materials gave higher levels of FM loss. This is due to the effects of pinning of domain walls by induced defects. From ac studies, we found that FM loss is independent of the ac frequency applied and it decreases drastically when the alloy is biased into its reversible regime by a collinear dc bias field. For fully coated tapes (with no effective “grooving”),

¹ In a configuration with the applied magnetic field H_{app} oriented *perpendicular* to the plane of the substrate, the magnetic response is strongly affected by its shape-dependent “effective” demagnetizing factor D . Qualitatively, the effective magnetizing field H_{eff} is reduced in magnitude relative to H_{app} , where $H_{\text{eff}} \approx [H_{\text{app}} - 4\pi D M_{\text{vol}}]$ and M_{vol} is the magnetic moment/volume; consequently the magnetization and hysteretic loss processes are spread over a wider range of applied fields, as illustrated for Ni metal in Ref. [11]. In the still more complex situation of some device (generator, transmission line, motor, ...) fabricated with tapes of coated conductor, quantitative estimates of total ac loss will likely require finite element (or equivalent) analysis. Note, however, that the *largest* FM loss/cycle (with large ac fields of *any* orientation) is given by the “saturation” values in Fig. 6, and the text estimates use values very near saturation. Thus the estimates presented represent the “worst case scenario” for ferromagnetic loss in the selected material.

estimates of the ac loss show that the ferromagnetic loss can be relatively small compared with that in the superconductor, for realistic levels of operating currents that are a significant fraction of the critical current.

Acknowledgements

We wish to thank Paul Barnes, D.K. Christen, R. Duckworth, H.R. Kerchner, and D.T. Verebelyi for informative discussions. Work at the University of Tennessee was supported by Air Force Office of Scientific Research Grant F49620-02-1-0182. The Oak Ridge National Laboratory is managed by UT-Battelle, LLC for the United States Department of Energy under contract no. DE-AC05-00OR22725.

References

- [1] A. Goyal, D.P. Norton, J.D. Budai, M. Paranthaman, E.D. Specht, D.M. Kroeger, D.K. Christen, Q. He, B. Saffian, F.A. List, D.F. Lee, P.M. Martin, C.E. Klabunde, E. Hatfield, V.K. Sikka, *Appl. Phys. Lett.* 69 (1996) 1795.
- [2] A. Goyal, J. Budai, D.M. Kroeger, D. Norton, E.D. Specht, D.K. Christen, US Patents: 5,739,086 (April 14, 1998); 5,741,377 (April 21, 1998); 5,898,020 (April 27, 1999); 5,958,599 (September 28, 1999).
- [3] A. Goyal, R. Feenstra, F.A. List, M. Paranthaman, D.F. Lee, D.M. Kroeger, D.B. Beach, J.S. Morrell, T.G. Chirayil, D.T. Verebelyi, X. Cui, E.D. Specht, D.K. Christen, P.M. Martin, *J. Metals* 51 (1999) 19.
- [4] M.W. Rupich, U. Schoop, D.T. Verebelyi, C. Thieme, W. Zhang, X. Li, T. Kodenkandath, N. Nguyen, E. Siegal, D. Buczek, J. Lynch, M. Jowett, E. Thompson, J.-S. Wang, J. Scudiere, A.P. Malozemoff, Q. Li, S. Annavarapu, S. Cui, L. Fritzscheier, B. Aldrich, C. Craven, F. Niu, A. Goyal, M. Paranthaman, *IEEE Trans. Appl. Supercond.* 13 (2003) 2459.
- [5] Y. Iijima, N. Tanabe, O. Kohno, Y. Ikeno, *Appl. Phys. Lett.* 60 (1992) 769.
- [6] Y. Iijima, K. Onabe, N. Futaki, N. Sadakata, O. Kohno, *J. Appl. Phys.* 74 (1993) 1905.
- [7] R.P. Reade, P. Berdahl, R.E. Russo, S.M. Garrison, *Appl. Phys. Lett.* 74 (1993) 2231.
- [8] X.D. Wu, S.R. Foltyn, P.N. Arendt, W.R. Blumenthal, I.H. Campell, J.D. Cotton, J.Y. Coulter, W.L. Hulst, M.P. Maley, H.F. Safar, J.L. Smith, *Appl. Phys. Lett.* 67 (1995) 2397.
- [9] K. Hasegawa, H. Fujino, H. Mukai, M. Konishi, K. Hayashi, K. Sato, S. Honjo, Y. Sato, H. Ishii, Y. Iwata, *Appl. Supercond.* 4 (1996) 487.
- [10] M. Fukutomi, S. Aoki, K. Kimori, R. Chatterjee, K. Togano, H. Maeda, *Physica C* 231 (1994) 113.
- [11] J.R. Thompson, A. Goyal, D.K. Christen, D.M. Kroeger, *Physica C* 370 (2001) 169.
- [12] A. Goyal, R. Feenstra, M. Paranthaman, J.R. Thompson, B.W. Kang, C. Cantoni, D.F. Lee, F.A. List, P.M. Martin, E. Lara-Curzio, C. Stevens, D.M. Kroeger, M. Kowalewski, E.D. Specht, T. Aytug, S. Sathyamurthy, R.K. Williams, R.E. Ericson, *Physica C* 382 (2002) 251.
- [13] R.C. Duckworth, J.R. Thompson, M.J. Gouge, J.W. Lue, A.O. Ijaduola, D. Yu, D.T. Verebelyi, *Supercond. Sci. Technol.* 16 (2003) 1294.
- [14] M.J. Besnus, Y. Gottehrer, G. Munshy, *Phys. Stat. Sol. B* 49 (1972) 597.
- [15] V. Marian, *Ann. Phys. Ser.* 11 (7) (1937) 459.
- [16] R.P. Bozorth (Ed.), *Ferromagnetism*, IEEE Press, Piscataway, NJ, 1978, p. 325.
- [17] M. Shiga (Ed.), *Landolt-Boernstein New Series Group III, Magnetic Properties of Metals*, vol. 19a, Springer-Verlag, Berlin, 1989, p. 563.
- [18] N.W. Ashcroft, N.D. Mermin, *Solid State Physics*, Holt, Rinehart and Winston, New York, 1976, p. 699.
- [19] V.A. Demkin, *Phys. Stat. Sol. (a)* 128 (1991) 375.
- [20] C. Park, D.P. Norton, J.D. Budai, D.K. Christen, D. Verebelyi, R. Feenstra, D.F. Lee, A. Goyal, D.M. Kroeger, M. Paranthaman, *Appl. Phys. Lett.* 73 (1998) 1904.
- [21] C.L.H. Thieme, E. Fleshler, D.M. Buczek, M. Jowett, L.G. Fritzscheier, P.N. Arendt, S.R. Foltyn, J.Y. Coulter, J.O. Willis, *IEEE Trans. Appl. Supercond.* 9 (1999) 1494.
- [22] J.R. Clem, A. Sanchez, *Phys. Rev. B* 50 (1994) 9355.
- [23] W.T. Norris, *J. Phys. D* 3 (1970) 489.
- [24] H.R. Kerchner, D.P. Norton, A. Goyal, J.D. Budai, D.K. Christen, D.M. Kroeger, E.D. Specht, Q. He, M. Paranthaman, D.F. Lee, B.C. Sales, F.A. List, R. Feenstra, *Appl. Phys. Lett.* 71 (1997) 2029.
- [25] M. Ciszek, O. Tsukamoto, N. Amemiya, J. Ogawa, O. Kasuu, H. Ii, K. Takeda, M. Shibuya, *IEEE Trans. Appl. Supercond.* 10 (2000) 1138.